Brain, Behavior, & Immunity - Health 8 (2020) 100128

Contents lists available at ScienceDirect

Brain, Behavior, & Immunity - Health

journal homepage: www.editorialmanager.com/bbih/default.aspx

Full Length Article

Urolithin-A attenuates neurotoxoplasmosis and alters innate response towards predator odor

Sijie Tan *, Wen Han Tong, Ajai Vyas

School of Biological Sciences, Nanyang Technological University, Singapore, 637551, Singapore

ARTICLE INFO

Keywords:
Behavioral manipulation
Brain
Cyst
Pomegranate extract
Toxoplasma gondii
Toxoplasmosis
Urolithin-A

ABSTRACT

Neurotoxoplasmosis, also known as cerebral toxoplasmosis, is an opportunistic chronic infection caused by the persistence of parasite *Toxoplasma gondii* cysts in the brain. In wild animals, chronic infection is associated with behavioral manipulation evident by an altered risk perception towards predators. In humans, reactivation of cysts and conversion of quiescent parasites into highly invasive tachyzoites is a significant cause of mortality in immunocompromised patients. However, the current standard therapy for toxoplasmosis is not well tolerated and is ineffective against the parasite cysts. In recent years, the concept of dietary supplementation with natural products derived from plants has gained popularity as a natural remedy for brain disorders. Notably, urolithin-A, a metabolite produced in the gut following consumption of ellagitannins-enriched food such as pomegranate, is reported to be blood-brain barrier permeable and exhibits neuroprotective effects *in-vivo*. In this study, we investigated the potential of pomegranate extract and urolithin-A as anti-neurotoxoplasmosis agents *in-vitro* and *in-vivo*. Treatment with pomegranate extract and urolithin-A reduced the parasite tachyzoite load and interfered with cyst development in differentiated human neural culture. Administration of urolithin-A also resulted in the formation of smaller brain cysts in chronically infected mice. Interestingly, this phenomenon was mirrored by an enhanced risk perception of the UA-treated infected mice towards predatory cues. Together, our findings demonstrate the potential of dietary supplementation with urolithin-A-enriched food as a novel natural remedy for the treatment of acute and chronic neurotoxoplasmosis.

1. Introduction

Infection by the protozoan parasite *Toxoplasma gondii* (*T. gondii*) is widely prevalent in animals as well as in humans (Tenter et al., 2000; Dubey, 2016; McLeod et al., 2020; Lindsay and Dubey, 2020). Members of the Felidae family are the only known definitive hosts for *T. gondii*, where the parasite completes the sexual phase of its reproduction in the intestine to form highly stable oocysts that are excreted (Frenkel et al., 1970; Miller et al., 1972). Humans are one of the intermediate hosts and often acquire the infection through ingestion of food contaminated with oocysts (Kijlstra and Jongert, 2008; Guo et al., 2015). Prenatal infection can also occur via vertical transmission from infected mother to fetus during pregnancy (Torgerson and Mastroiacovo, 2013). Depending on the geographical region, the prevalence of toxoplasmosis varies, although it is estimated that a third of the world's human population is chronically infected (McLeod et al., 2020; Molan et al., 2019).

T. gondii exists in two stages in humans and all intermediate hosts. Once ingested, sporozoites released from the oocysts are converted to the highly replicating invasive tachyzoites that disseminate in all organs, causing an acute infection (Dubey et al., 1998; Dubey, 2020). The tachyzoites then differentiate into slow-growing bradyzoites, forming quiescent tissue cysts, and establishing chronic infection in the hosts (Dubey et al., 1998; Dubey, 2020). The encystment of *T. gondii* bradyzoites displays strong tropism for the brain and exhibits a distinct propensity for the neurons (Remington and Cavanaugh, 1965; Ferguson and Hutchison, 1987; Koshy et al., 2010, 2020; Melzer et al., 2010; Cabral et al., 2016). Encysted parasites can reside for a prolonged period in the brain and avoid immune-related destruction or clearance (Sullivan and Jeffers, 2012; Jeffers et al., 2018). These cysts intermittently rupture, releasing bradyzoites which can differentiate into invasive tachyzoites (Dubey et al., 1998; Dubey, 2020; Ferguson et al., 1989; Frenkel and Escajadillo, 1987). Chronic infection has been associated with altered cognition and behavior in intermediate hosts (Webster, 2001; Parlog et al., 2015). A well-reported change by *T. gondii* infection pertains to behavioral alteration in rodents, where chronically infected animals display general loss of innate fear towards felid predators (Berdoy et al.,

* Corresponding author. School of Biological Sciences, Nanyang Technological University, SBS-02n-10, 60 Nanyang Drive, Singapore, 637551, Singapore.
E-mail address: sjtan@ntu.edu.sg (S. Tan).

https://doi.org/10.1016/j.bbih.2020.100128
Received 21 May 2020; Received in revised form 4 August 2020; Accepted 7 August 2020
Available online 11 August 2020

2000; Vyas et al., 2007; Vyas, 2015). The severity of the behavioral alteration is also shown to correlate with the brain cyst burden (Afonso et al., 2012; Evans et al., 2014; Xiao et al., 2016; Boillat et al., 2020). In humans, much of the attention relating to the pathology of *T. gondii* infection has also focused on the brain. Compelling evidence over the years has raised awareness of chronic cerebral toxoplasmosis as a possible risk factor for the development of neurological and psychiatric disorders (Fabiani et al., 2015; Severance et al., 2016; Tyebji et al., 2019). Particularly in immunocompromised patients, reactivated cysts cause severe morbidity and mortality (Nissapatorn et al., 2004), prompting efforts to identify remedies that can mitigate cerebral toxoplasmosis.

An ideal drug for cerebral toxoplasmosis should be permeable to the blood-brain barrier and is effective against both the replicating tachyzoites and the quiescent bradyzoites within tissue cysts. Additionally, the drug should exhibit high oral bioavailability and is inexpensive to produce. Currently, the treatment regimen for toxoplasmosis involves the combination of antifolates pyrimethamine and sulfadiazine to inhibit *T. gondii* growth (Dunay et al., 2018). However, these drugs exhibit side-effects and are poorly tolerated in immunocompromised patients (Dunay et al., 2018; Porter and Sande, 1992; Dannemann et al., 1992; Katlama et al., 1996). The rising cost of pyrimethamine coupled with the need for a prolonged course of treatment also makes the current treatment regimen expensive to patients (McCarthy, 2015). More importantly, the unique pathogenesis of *T. gondii* presented a challenge for the current therapy; these drugs are only capable of suppressing the tachyzoite stage and are ineffective against the encysted bradyzoites (Dunay et al., 2018; Alday and Doggett, 2017). Thus, the identification of new therapeutic alternatives that are safer, cheaper, and effective against the parasite cysts would greatly improve the care of patients with toxoplasmosis.

In recent years, the identification of natural products derived from plants and herbs with antimicrobial activity has intensified (Farha and Brown, 2016; Gyawali and Ibrahim, 2014). Indeed, multiple studies have demonstrated the potential of natural plant products as an alternative to standard drug therapy against toxoplasmosis (Sepulveda-Arias et al., 2014; Al Nasr et al., 2016; Arab-Mazar et al., 2017; Deng et al., 2019; Adeyemi et al., 2019). The pomegranate fruit is a rich source of ellagitannins, a class of natural polyphenols that are metabolized to urolithins by gut microbiota (Espin et al., 2013). While the bioavailability of ellagitannins is low, urolithins are well-absorbed and can reach wide tissue targets (Espin et al., 2013; Cerdá et al., 2003, 2004; Seeram et al., 2006; Mertens-Talcott et al., 2006). Specifically, urolithin-A (UA) is reported to persist in the blood plasma following the consumption of pomegranate extract (PE) in humans (Mertens-Talcott et al., 2006). Thus, UA is widely regarded as the bioactive molecule underlying the health benefits of pomegranate consumption. More importantly, UA can cross the blood-brain barrier and has been shown to be a powerful neuroprotectant *in-vivo* against Alzheimer's and Parkinson's Disease, ischemic neuronal injury, and brain aging (Gasperotti et al., 2015; Ryu et al., 2016; Yuan et al., 2016; Ahsan et al., 2019; Gong et al., 2019; Andreux et al., 2019; Chen et al., 2019; Kujawska et al., 2020).

Given the compelling evidence supporting the neuroprotective properties of UA against brain disorders, we posit the administration of PE and UA could mitigate cerebral toxoplasmosis. Using the differentiated human neural culture and the murine chronic toxoplasmosis model, we investigated how the administration of PE and its bioactive metabolite UA influence the parasite load *in-vitro* and *in-vivo*. More importantly, we looked at how treatment with UA modulates *T. gondii* cyst development. Since behavioral alternation is associated with the brain cyst burden (Afonso et al., 2012; Evans et al., 2014; Xiao et al., 2016; Boillat et al., 2020), we also examined whether UA could potentially affect the risk perception of infected mice towards predatory cat odor. In summary, supported by the cellular and behavioral evidence from our *in-vitro* and *in-vivo* toxoplasmosis models, our study aimed to identify the potential of dietary supplementation with UA-enriched food as a natural remedy for acute and chronic cerebral toxoplasmosis.

2. Materials and methods

2.1. Ethics statements

All animal procedures were carried out in strict accordance with the guidelines from the National Advisory Committee for Laboratory Animal Research (NACLAR). The protocol was approved by the Institutional Animal Care and Use Committee (IACUC) at Nanyang Technological University, Singapore (# A19046).

2.2. Culturing and differentiation of human ReNcell VM neural progenitor cells

The immortalized human ReNcell VM (Ventral Mesencephalon) neural progenitor cells (EMD Millipore) were cultured on 20 μg/ml laminin-coated plates (Corning), in Dulbecco's Modified Eagle Medium (DMEM): Nutrient Mixture F12 (DMEM/F12) media (Life Technologies) supplemented with 2% (v/v) B27 neural supplement (Life Technologies), 2 μg/ml heparin (StemCell Technologies), 20 μg/ml human Epidermal Growth Factor (EGF; Sigma), 20 μg/ml human Fibroblast Growth Factor-basic (bFGF; Life Technologies), and 100 units/ml penicillin-streptomycin solution (GE Hyclone). The culture media was changed every 3 days until the cells were confluent and ready for subculturing. Differentiation of the neural progenitor cells was initiated by replacing the culture media with DMEM/F12 supplemented with 2% (v/v) B27 neural supplement, 2 μg/ml heparin, and 100 units/ml penicillin-streptomycin solution without the growth factors EGF and bFGF. The differentiation media was changed every 3 days for 3–4 weeks. All cells were grown in 5% CO_2 at 37 °C.

2.3. Toxoplasma strains and maintenance

Wild-type type II Prugniaud (Pru) and transgenic Green Fluorescent Protein (GFP)-expressing Pru *T. gondii* strains (Vyas et al., 2007) were maintained by serial passage on monolayers of Human Foreskin Fibroblast (HFF) (ATCC) cultured in DMEM (Life Technologies) supplemented with 10% (v/v) Fetal Bovine Serum (FBS) (GE Hyclone) and 100 units/ml penicillin-streptomycin solution. Briefly, adherent *T. gondii*-infected HFF monolayers were trypsinized (0.25% trypsin; ThermoFisher Scientific) and lysed by passing through a 25-G needle for 10 times to release the intracellular parasites. Parasite count was determined with the hemocytometer. Cells and parasites were grown in 5% CO_2 at 37 °C.

2.4. Preparation of urolithin-A and pomegranate extract

For the treatment of differentiated ReNcell, UA (Tocris Bioscience) and Pomella® PE (Verdure Sciences) were dissolved in Dimethyl Sulfoxide (DMSO) to yield a stock concentration of 10 mM and 5 mg/ml respectively. Final working concentrations of UA (50 μM and 100 μM) and PE (300 μg/ml) were reconstituted by diluting the stocks in the differentiation media. For intraperitoneal injection in mice, 50 mg of UA was first dissolved in DMSO and then further diluted in 1x Phosphate-Buffered Saline (PBS) (Sigma). Each animal was administered 30 μg UA in 100 μl of 1x PBS. For both *in-vitro* and *in-vivo* work, the equivalent volume of DMSO was used as vehicle control.

2.5. T. gondii infection and treatments in differentiated ReNcell cells

Differentiated ReNcell were infected with wild-type (for cell viability assays) or GFP-Pru (for parasite and cyst burden assays) *T. gondii* strain at Multiplicity of Infection (MOI) 1 for 24 h. To examine the effects of PE or UA on the intracellular parasites, the differentiation media was replaced with new media containing the respective concentration of UA, PE, or the equivalent volume of DMSO post-infection for another 24 h.

2.6. Imaging total T. gondii burden in differentiated ReNcell cells

48 h post-infection and treatment, infected cells on coverslips were fixed with 4% paraformaldehyde (PFA) (Sigma) at 37 °C for 20 min. The coverslips were mounted onto a glass slide with ProLong Gold Antifade Mountant containing DAPI (4', 6-diamidino-2-phenylindole; Life Technologies). Cells were immediately imaged with the Zeiss Z1 Axio Observer inverted fluorescence microscope (Zeiss) using the 40x objective lens with a 1.2x digital magnification. 10 random fields per coverslip were imaged and the same acquisition parameters were applied to all treatment groups for a fair comparison. *Image J* program was used to quantify the total parasite burden using fluorescence emanating from GFP transgene inserted within the parasite. A consistent threshold value was applied across all images and the total area of the GFP signals was normalized to the total number of DAPI nuclei.

2.7. RNA extraction, reverse transcription, and quantitative real-time PCR (qPCR)

RNA was extracted using the RNeasy Mini Kit (Qiagen) followed by DNase treatment with RQ1 RNase-Free DNase (Promega). 2 μg of isolated RNA was reverse transcribed using M-MLV Reverse Transcriptase (Promega) and amplified with GoTaq Flexi DNA Polymerase (Promega) for PCR-agarose gel analysis. qPCR was performed using the SYBR Select Master Mix (Life Technologies). All steps were performed according to the manufacturer's protocols.

The following primers were used for PCR: *SAG1* forward 5′-GGCTGTAACATTGAGCTCCTTGATTCCTGAAGCAGAAGATAGC-3'; *SAG1* reverse 5′-GCGTCATTATTGGATGCACAGGGGGATCGCCTGAGAAGCATCAC-3'; *β-actin* forward 5′-CCAGAGGCGTACAGGGATAG-3'; *β-actin* reverse 5′-CCAACCGCGAGAAGATGA-3'. The following primers were used for qPCR: *SAG1* forward 5′-TTAAGTGAGAACCCGTGGCAG-3'; *SAG1* reverse 5′-GCTTTTTGACTCGGCTGGAA-3'; *GAPDH* forward 5′-GACCACAGTCCATGCCATCACTGCC-3'; *GAPDH* reverse 5′-GCCTGCTTCACCACCTTCTTGATG-3'.

2.8. Cell viability: neurite outgrowth staining assay and MTS assay

In-vitro cytotoxicity of *T. gondii*-infected cells post-treatment was determined with the neurite outgrowth staining kit (Life Technologies) and MTS assay (Sigma) according to the manufacturer's protocols. Briefly, cells were washed with 1x PBS. For the neurite outgrowth staining kit, 1x Cell Viability Indicator and 1x Cell Membrane Stain were reconstituted in 1x PBS containing Ca^{2+} and Mg^{2+} (Life Technologies) and added to each well. The cells were incubated with the stain solution at 37 °C for 20 min. Following this, the stain solution was removed, and the cells were rinsed with 1x PBS. 1x Background Suppression Dye reconstituted in 1x PBS containing Ca^{2+} and Mg^{2+} was added to each well, and the cells were immediately imaged with the Zeiss Z1 Axio Observer inverted fluorescence microscope using the 10x objective lens with a 1.2x digital magnification. The FITC filter set was used for imaging the Cell Viability Indicator (green) and the TRITC filter set was used for the Cell Membrane Stain (Red). 6–8 random fields per well were imaged and the same acquisition parameters were applied to all treatment groups. Cell viability was expressed as the ratio of the green to the red signal area, which indicates the proportion of viable cells (green) over the total cell population (red). *Image J* was used to quantify the green and red signal areas as described earlier. For the MTS assay, MTS reagent at 1:10 dilution was concocted in 1x PBS containing Ca^{2+} and Mg^{2+} and added to each well. The cells were incubated with the MTS reagent at 37 °C for 4 h. The absorbance (Abs) was immediately measured with the Tecan Infinite M200 Pro spectrophotometer (Tecan) at OD = 490 nm. Triplicates were performed for each treatment condition and the average Abs value was calculated. The final Abs value used for tabulation of cell viability takes into account the average reading from the control wells without the MTS reagent (cell viability = $Abs_{treatment} - Abs_{control}$).

2.9. T. gondii infection and UA injection in mice

7-weeks old BALB/cJInv female mice (InVivos Pte Ltd) were acclimatized to the vivarium (12:12 light-dark cycle, lights on at 07:00 h) for 1 week before the start of intraperitoneal injections. On the first day, all animals were infected with 200 freshly syringe-released GFP-Pru *T. gondii* reconstituted in 100 μl 1x PBS. 2-days post-infection, each animal was injected daily with either 30 μg freshly reconstituted UA or equivalent volume of DMSO in 100 μl 1x PBS up till 5 weeks. Food and water were available ad libitum throughout the experiment.

2.10. Bobcat urine aversion assay

The response to bobcat urine was assessed 5-weeks post-injection, using a previously published experimental paradigm (Boillat et al., 2020). The behavioral runs were conducted in a rectangular arena divided into two opposing and identical bisects. Mice were habituated once a day for 3 consecutive days and tested on the 4th day. For habituation, the mice were individually placed in the arena and allowed to explore for 15 min. On the test day, a petri dish containing beddings from the homecage was placed at one end of the arena and the animal was allowed to explore for 5 min (pre-exposure phase). The animal was then confined to the bisect containing the homecage beddings by placing a temporary insert in the middle of the arena. A small piece of paper towel spotted with 1 mL of pure bobcat urine (Maine Outdoor Solutions) was clipped onto the wall of the opposite bisect. The temporary insert was removed, and the behavior of the animal was recorded for 10 min (exposure phase). All behaviors were analyzed by the experimenter and an observer blind to the conditions. The time spent in each bisect was quantified and the aversion index was calculated as followed: $Time_{\text{bobcat urine bisect}}/Time_{\text{homecage beddings bisect}}$.

2.11. In-vitro and in-vivo cyst burden

To determine the cyst size *in-vitro*, infected cells on coverslips were fixed with 4% PFA for 20 min and blocked for 1 h (recipe for blocking buffer: 1x PBS containing 5% (w/v) Bovine Serum Albumin (BSA) (Sigma) with 0.5% (v/v) Triton X-100 (Sigma)). Subsequently, the cells were incubated with biotinylated *anti-Dolichos biflorus agglutinin* (DBA) at 1:250 dilution (Vector Laboratories) in the blocking buffer for 3 h. The cells were washed in 1x PBS and incubated with the blocking buffer containing Alexa Fluor 555 streptavidin secondary antibody (1:1000 dilution; Life Technologies) for 1 h. The cells were washed with 1x PBS and the coverslips were mounted onto a glass slide with DAPI. The entire process was performed at room temperature.

To determine the cyst burden *in-vivo*, the mice were immediately sacrificed upon completion of the bobcat urine aversion assay. The brains were collected and snap-frozen. Approximately half the brain (cut at the sagittal plane) was homogenized in 2 ml 1x PBS by pressing through a 100 μm-pore nylon cell strainer (Sigma) using the plunger of a 5 ml syringe. 2 ml of the 1x lysis buffer concoction in 1x PBS (recipe for 5x lysis buffer: 10 mM Tris, 1 mM EDTA, 0.2% (w/v) SDS, and 10 mM NaCl, top up with distilled water, pH adjusted to 8.0)) supplemented with 0.008 units/ml proteinase K (ThermoFisher Scientific) was added to the flow-through (brain homogenate) and incubated at 56 °C for 15 min. The sample was pelleted and resuspended in 1 ml blocking buffer. Biotinylated *anti-DBA* at 1:250 dilution was incubated with the brain homogenate at room temperature on a mechanical wheel for 3 h. The sample was then pelleted, washed with 1x PBS, and resuspended in 1 ml blocking buffer containing Alexa Fluor 555 streptavidin secondary antibody (1:1000 dilution). The sample was incubated at room temperature on a mechanical wheel in the dark for 1 h, pelleted, washed with 1x PBS, and pelleted again. All centrifugation/pelleting steps were conducted at room temperature, 1,250 *g* for 15 min. The pellet containing the stained cysts was resuspended in 200 μl 1x PBS and a 50 μl aliquot was smeared onto a glass slide (giving a total of 4 smeared slides). A glass slip was

layered on top of the smear and the slides were dried.

The slides were scanned for cysts using the Zeiss Z1 Axio Observer inverted fluorescence microscope using the 10x objective lens with a 1.2x digital magnification. For the *in-vitro* cyst burden, the number of cysts counted was normalized to the total nuclei count. For the *in-vivo* smear slides, the number of cysts counted across the 4 smears was normalized against the weight of the half brain. To quantify the size of the cysts, cyst images were acquired using the 40x objective lens at 1.2x digital magnification. *Image J* program was used to highlight the cyst and the diameter was determined.

2.12. Statistical analyses

All statistical analyses were performed using GraphPad Prism 5 (GraphPad Software, Inc.). Statistical tests for any given set of data were described in the figure legends. In brief, for direct comparison between a single treatment group against the DMSO control, a two-tailed t-test was used. For comparison between multiple treatment groups, Kruskal-Wallis test, one-way ANOVA followed by Dunnett's multiple comparisons test, or one-way ANOVA followed by Tukey's multiple comparison test was used. Results are always presented as mean ± S.E.M. Significance are $*p \leq 0.05$, $**p \leq 0.001$, $***p \leq 0.0001$. The details of all statistical analyses can be found in Table S1.

3. Results

3.1. In-vitro T. gondii replication and spontaneous cyst formation in differentiated neural cells

To model and examine neurotoxoplasmosis *in-vitro*, we differentiated the human neural progenitor ReNcell VM cells, a neural stem cell line derived from the ventral mesencephalic region of the developing brain, and infected the cells with GFP-Pru *T. gondii*. As previously reported (Hoffrogge et al., 2006; Donato et al., 2007; Choi et al., 2014), ReNcell progenitors differentiate into neuronal and glial cells within 3 weeks upon withdrawal of growth factors. Live imaging revealed morphological changes to the neural culture upon 4-weeks differentiation (Fig. 1a). qPCR showed a robust increase in neuronal (*MAP2, NCAM1, TUBB3*) and

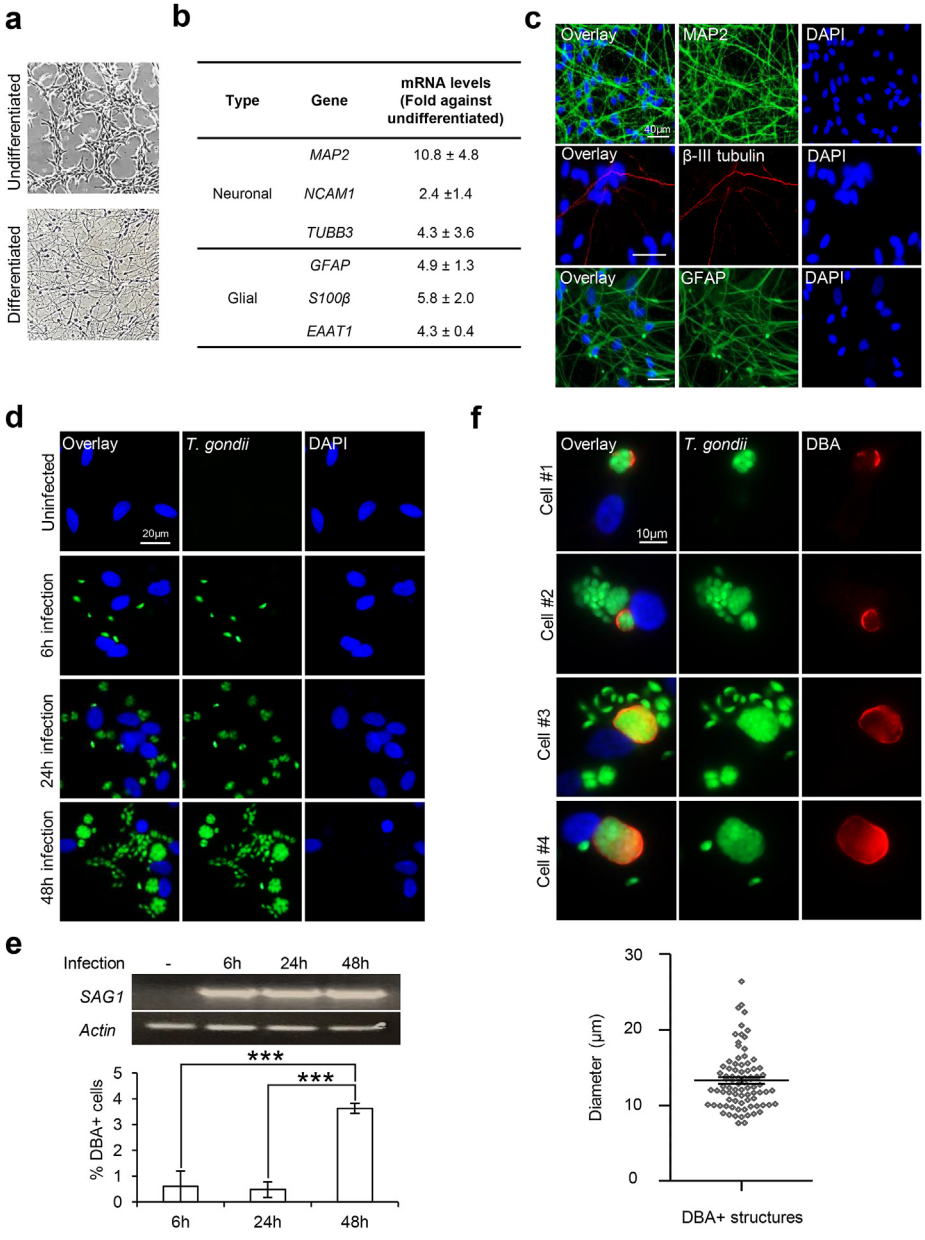

Fig. 1. *T. gondii* proliferation and cyst development in differentiated ReNcell neural cells. (a–c) Differentiation of human ReNcell VM neural progenitors upon removal of growth factors for 4 weeks. (a) Bright-field images of undifferentiated and differentiated ReNcell. (b) qPCR analysis of neuronal and glial cell markers in differentiated ReNcell. mRNA levels for each gene were normalized against *β-actin* and calculated as fold change against the undifferentiated control cells (n = 4–6). (c) Immunofluorescence images of MAP2, β-III tubulin, and GFAP in differentiated ReNcell. (d–f) 3-weeks differentiated ReNcell were infected with GFP-Pru *T. gondii* at MOI 1 for 6, 24, and 48 h. (d) Fluorescence images of GFP + *T. gondii* signals. (e) PCR for gene expression of *SAG1* (top) and percentage of cells with DBA + structure (bottom). 100–600 cells per experimental set (n = 6) were analyzed for the presence of DBA structure. (f) Representative images of 4 selected cells stained positive for DBA (top) and the diameter of DBA + structures (bottom) at 48 h infection. A total of 84 DBA + structures (one dot represents one structure) identified across 6 experimental sets (n = 6) were analyzed. The horizontal line represents the average diameter. Nuclei were stained with DAPI. All values are mean ± S.E.M. One-way ANOVA with Tukey's multiple comparison test was performed. Differences against 48 h are significant for $***p \leq 0.0001$. Scale bars: 10 μm (Fig. f), 20 μm (Fig. d), or 40 μm (Fig. c).

glial (*GFAP, S100β, EAAT1*) markers (Fig. 1b), and immunostaining with MAP2, β-III tubulin and GFAP (Fig. 1c) confirmed the protein expression. Next, differentiated ReNcell were infected with *T. gondii* at MOI 1 for 6, 24, and 48 h. Examination of the GFP-positive (+) *T. gondii* revealed an increase in parasite load over the course of the infection (Fig. 1d). To investigate whether infection of differentiated ReNcell could recapitulate *T. gondii* tachyzoite and cyst stage, we checked for the expression of tachyzoite-specific surface protein *SAG1* and stained for the glycosylated cyst wall using *anti-DBA*. The expression of *SAG1* was consistently observed across the infection period (Fig. 1e, top). Similarly, DBA + structures were also detected in the infected cells (Fig. 1e, bottom). However, the proportion DBA + cells were significantly higher with 48 h infection, with ~3.6% of the cells harboring cyst structures ($F = 27.78$, $R^2 = 0.8347$, $p < 0.0001$; Fig. 1e, bottom). Qualitative analysis of these structures revealed cyst size ~13.30 ± 0.41 μm in diameter (Fig. 1f). Together, our observations highlight the feasibility of *T. gondii*-infected differentiated ReNcell neural cells as an *in-vitro* neurotoxoplasmosis model to examine tachyzoite proliferation and cyst development. We also attempted to further prolong the infection in the hope of capturing higher *in-vitro* cyst load in the differentiated ReNcell. However, heavily infected neural culture was observed to lyse by 56 h post-infection. Hence, subsequent *in-vitro* experiments were conducted using the 48 h infection paradigm, the optimal duration which allows for the investigation of parasite replication and cyst formation without causing significant cytotoxicity to the host cells (Supplementary Fig. S1).

3.2. Pomegranate extract reduces parasite burden and cyst formation in-vitro

There is growing evidence supporting anti-*T. gondii* activity in natural polyphenols derived from plants (Sepulveda-Arias et al., 2014; Al Nasr et al., 2016; Arab-Mazar et al., 2017; Deng et al., 2019; Adeyemi et al., 2019). Hence, we were interested to investigate if PE, a polyphenols-enriched mixture, can target tachyzoite growth and cyst formation *in-vitro*. Differentiated ReNcell were first infected with GFP-Pru *T. gondii* for 24 h. To examine whether PE is active against intracellular parasites, 300 μg/ml PE or DMSO vehicle control was added to the infected cells post-infection for 24 h. Examination of the GFP + *T. gondii* revealed a significant reduction in the total parasite load by ~3 folds in PE-treated cells when compared to the DMSO control cells ($t_{(3)} = 39.63$, $p < 0.0001$; Fig. 2a). When we looked into the specific *T. gondii* developmental stages, qPCR of the *SAG1* gene showed that PE significantly reduced the *SAG1* mRNA levels by ~4.2 folds ($t_{(3)} = 12.58$, $p = 0.0011$; Fig. 2b). Examination of the DBA + structures also revealed a significant reduction in the percentage of DBA + cells from ~2.9% to 0.3% with PE treatment ($t_{(3)} = 10.67$, $p = 0.0018$; Fig. 2c). Together, these results demonstrate that PE targets *T. gondii* tachyzoite and bradyzoite forms to inhibit parasite growth and cyst formation in differentiated neural cells.

3.3. Urolithin-A reduces tachyzoite load and perturbs cyst formation in-vitro

UA is a gut microbiome-derived metabolite of ellagitannins, a class of bioactive polyphenols highly enriched in pomegranate (Espin et al., 2013). While ellagitannins have low bioavailability, the metabolite UA can persist in the blood plasma and possess the ability to cross the blood-brain barrier (Espin et al., 2013; Cerdá et al., 2003, 2004; Seeram et al., 2006; Mertens-Talcott et al., 2006; Gasperotti et al., 2015; Yuan et al., 2016). With the earlier findings (Fig. 2), we were interested to investigate whether UA is the bioactive compound underlying the *in-vitro* protective effect of PE against neurotoxoplasmosis. Differentiated

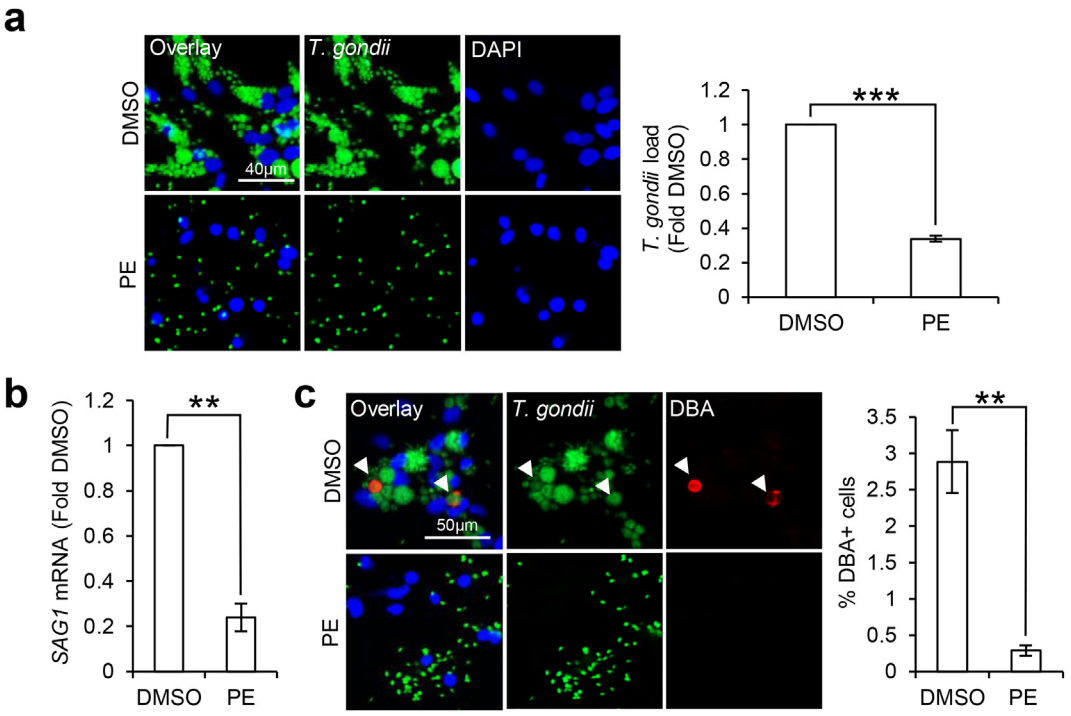

Fig. 2. Pomegranate extract reduces *T. gondii* tachyzoite and cyst formation in differentiated neural cells. 3-weeks differentiated neural cells were infected with GFP-Pru *T. gondii* at MOI 1 for 24 h followed by treatment with vehicle control DMSO or 300 μg/ml PE for 24 h. (a) Fluorescence images (left) and quantification (right) of GFP + *T. gondii* signals, calculated as fold change against DMSO control. 150–300 cells in each treatment group per experimental set (n = 4) were analyzed for the GFP signals. (b) qPCR for *SAG1* mRNA levels. mRNA levels were normalized against *GAPDH* and calculated as fold change against the DMSO control cells (n = 4). (c) Immunofluorescence images (left) and quantification (right) of percentage DBA + cells. White arrows indicate DBA + structures. 250–500 cells in each treatment group per experimental set (n = 4) were analyzed for the presence of DBA structure. Nuclei were stained with DAPI. All values are mean ± S.E.M. Two-tailed paired t-test with a 95% confidence interval was performed. Differences against DMSO control are significant for $^{**}p \leq 0.001$ and $^{***}p \leq 0.0001$. Scale bars: 40 μm (Fig. a) or 50 μm (Fig. c).

ReNcell were first infected with GFP-Pru *T. gondii* for 24 h followed by treatment with PE, 50 μM or 100 μM UA for another 24 h. Consistent with earlier finding (Fig. 2a), PE treatment reduced the total GFP + *T. gondii* load as compared to the DMSO control cells ($F_{(3,12)} = 38.81$, $p < 0.0001$; Fig. 3a). Likewise, treatment with 50 μM or 100 μM UA significantly lowered the parasite burden by ~1.8 and 2.7 folds respectively compared to the DMSO control ($F_{(3,12)} = 38.81$, $p < 0.0001$; Fig. 3a). qPCR analysis of *SAG1* revealed a trend consistent with the total parasite load, where treatment with PE or UA reduced the *SAG1* mRNA levels in *T. gondii*-infected differentiated neural cells ($F_{(3,20)} = 13.66$, $p < 0.0001$; Fig. 3b). Next, we assessed if UA also inhibits cyst formation. Examination of the percentage of DBA + cells revealed a moderate reduction in the cells containing cyst with UA treatment, especially at 100 μM concentration (*Kruskal-Wallis statistic* = 5.956, $p = 0.0509$; Fig. 3c). However, qualitative analysis of the DBA + structures showed that 50 μM and 100 μM UA treatment led to the appearance of smaller cysts with an average diameter of ~5.15 ± 0.18 μm and 9.44 ± 0.23 μm respectively as compared to ~14.04 ± 0.42 μm in DMSO control cells ($F_{(2,203)} = 132.7$, $p < 0.0001$; Fig. 3d). Together, our findings highlight UA as a potent anti-*T. gondii* compound that attenuates tachyzoite growth and cyst development in differentiated neural cells. In addition, we postulate that UA is the bioactive compound in PE that may in part, contribute to the biological activity of PE against toxoplasmosis.

3.4. Pomegranate extract and urolithin-A do not cause cytotoxicity in-vitro

T. gondii is an obligate intracellular parasite that requires the host cell for survival (Blader et al., 2015). Consequently, the death of the host cells also reduces *T. gondii* viability. It is important that a remedy against neurotoxoplasmosis can negate parasite burden without compromising neuronal health. To this end, we investigated if PE and UA reduced *T. gondii* load in differentiated neural cells (Figs. 2 and 3) as a consequence of cytotoxicity to the host cells. Cell viability of the infected cells treated with PE or UA was measured using the neurite outgrowth staining kit and MTS assay. The neurite outgrowth staining kit allows for visualization of viable cells (green) and the total cell population (red) to provide an indication of the cell viability (green: red ratio). Examination of the green to red signal ratio revealed that PE and UA did not significantly alter the viability of the infected neural cells as compared to the DMSO control ($F_{(3,12)} = 0.9214$, $p = 0.46$; Fig. 4a). This finding was consistent with the observations from the MTS assay, where PE and UA did not induce significant changes to the cell viability ($F_{(3,16)} = 0.9368$, $p = 0.9368$; Fig. 4b). Together, these results highlight that the reduction in parasite burden by PE and UA was not due to cytotoxicity to the host cells.

3.5. Urolithin-A inhibits cyst formation in-vivo and alters the innate response of infected mice towards predatory cat odor

With the earlier observations supporting the neuroprotective role of UA against *T. gondii* tachyzoite growth and more importantly, the formation of cysts in differentiated neural culture *in-vitro* (Fig. 3), we investigated if UA could similarly attenuate neurotoxoplasmosis *in-vivo*. To concurrently examine both the tachyzoite and cyst load, mice were first intraperitoneally injected with the GFP-Pru *T. gondii* (Fig. 5a). 2-days post-infection, the animals were administered with either 30 μg UA or an equivalent volume of DMSO daily (Fig. 5a). To attain chronic infection and evaluate cyst formation, the mice were sacrificed 39-days (~5.5 weeks) post-infection (Fig. 5a). The brains were harvested and examined for the tachyzoite and cyst load. First, we observed that 40% of the infected DMSO control mice succumbed to acute infection and died 10-days post-infection, whereas UA-injected mice survived through the experimental duration (Supplementary Fig. S2a). This suggests moderate protection by UA against lethal acute infection. Next, we examined the

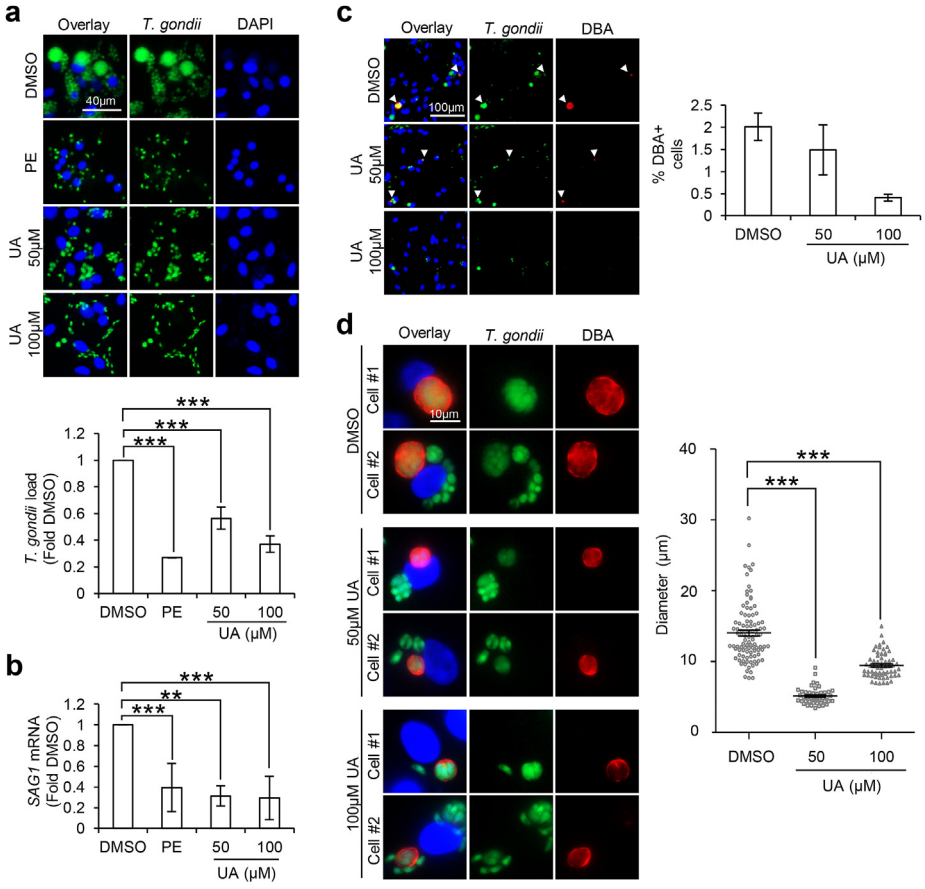

Fig. 3. Urolithin-A reduces *T. gondii* tachyzoite load and leads to the formation of smaller cysts in differentiated neural cells. 3-weeks differentiated neural cells were infected with GFP-Pru *T. gondii* at MOI 1 for 24 h followed by treatment with vehicle control DMSO, 300 μg/ml PE, 50 μM or 100 μM UA for 24 h. (a) Fluorescence images (top) and quantification (bottom) of GFP + *T. gondii* signals, calculated as fold change against DMSO control. 150–300 cells in each treatment group per experimental set (n = 4) were analyzed for the GFP signals. (b) qPCR for *SAG1* mRNA levels. mRNA levels were normalized against *GAPDH* and calculated as fold change against the DMSO control (n = 3–9). (c) Immunofluorescence images (left) and quantification (right) of percentage DBA + cells. White arrows indicate DBA + structures. 250–450 cells in each treatment group per experimental set (n = 3) were analyzed for the presence of DBA structure. (d) Representative images of 2 selected DBA + infected cells in each treatment group (left) and diameter (right) of the DBA + structures. A total of 99 (DMSO), 45 (50 μM UA) and 62 (100 μM UA) DBA + structures (one dot represents one structure) identified across 3 experimental sets (n = 3) were analyzed. The horizontal line represents the average diameter. Nuclei were stained with DAPI. All values are mean ± S.E.M. One-way ANOVA with Dunnett's multiple comparisons test (DMSO set as the control) or Kruskal-Wallis test was performed. Differences against DMSO are significant for $^{**}p \leq 0.001$ and $^{***}p \leq 0.0001$. Scale bars: 10 μm (Fig. d), 40 μm (Fig. a) or 100 μm (Fig. c).

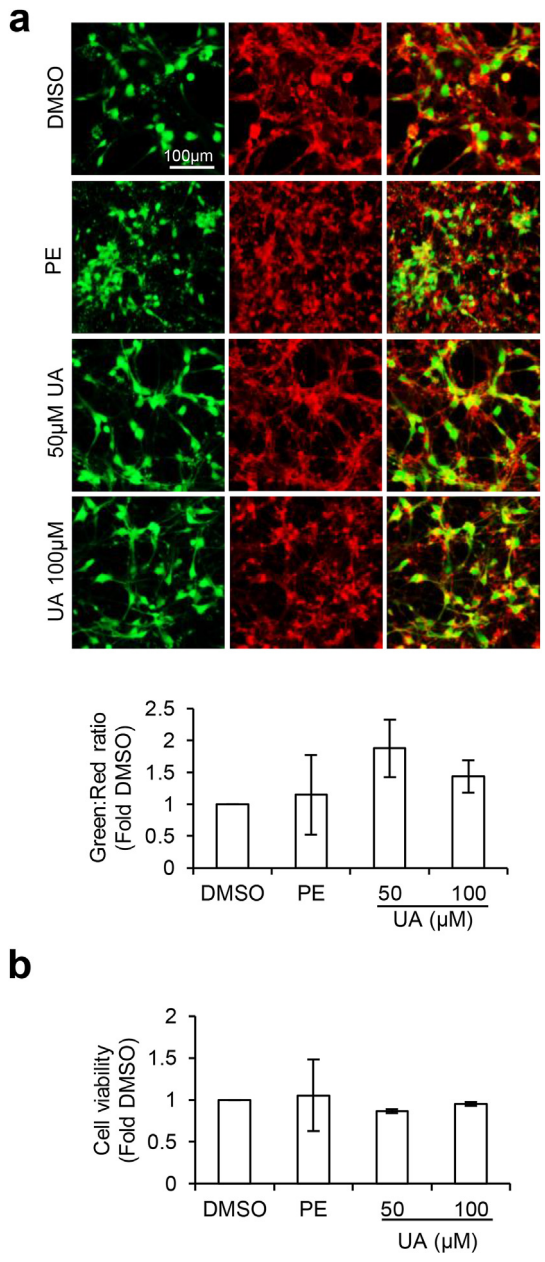

Fig. 4. Pomegranate extract and urolithin-A do not induce cell death. 3-weeks differentiated neural cells were infected with Pru *T. gondii* at MOI 1 for 24 h followed by treatment with vehicle control DMSO, 300 μg/ml PE, 50 μM or 100 μM UA for 24 h. (a) Neurite outgrowth staining kit to assess cell viability. Fluorescence images (top) and quantification (bottom) of green (viable cells) to red (total cells) signal ratio (n = 4). (b) MTS assay to quantify cell viability. The graphs were plotted as fold change against DMSO control (n = 5). All values are mean ± S.E.M. One-way ANOVA with Dunnett's multiple comparisons test (DMSO set as the control) was performed. Scale bar: 100 μm. (For interpretation of the references to colour in this figure legend, the reader is referred to the Web version of this article.)

tachyzoite load in the brains of the infected mice that survived until the end of the experiment. Interestingly, negligible *SAG1* expression was detected in both the DMSO and UA-injected mice (Supplementary Fig. S2b). We postulate that at the stage of chronic infection, *T. gondii* may have encysted, resulting in low tachyzoite form in the brain. Lastly, we assessed the cyst load in the brains of the chronically infected animals. Quantification of the DBA + structures revealed only a mild reduction in the cyst count in the UA-injected mice compared to the control mice ($t_{(8)} = 1.174$, $p = 0.2743$; Fig. 5c). However, qualitative analysis of the cyst size showed that UA mice have significantly smaller cyst diameter than the DMSO mice ($t_{(250)} = 3.167$, $p = 0.0017$; Fig. 5b and 5d). This observation on cyst size was consistent with the *in-vitro* findings (Fig. 3d), demonstrating that UA interferes with cyst formation.

One of the most widely regarded effect of *T. gondii* on rodent behavior is the unusual attraction to cat odor in chronically infected animals (Berdoy et al., 2000; Vyas et al., 2007). Notably, this behavioral manipulation appears to correlate with the severity of the cyst burden in the brain (Afonso et al., 2012; Evans et al., 2014; Xiao et al., 2016; Boillat et al., 2020). With the earlier findings demonstrating the inhibitory effect of UA on cyst formation *in-vitro* and *in-vivo* (Figs. 3d and 5d), we evaluated whether UA administration could alter the response of infected mice towards cat odor. To this end, we conducted the bobcat urine aversion assay modified from the paradigm reported earlier (Boillat et al., 2020). This assay was conducted using the same batch of chronically infected mice assessed for cyst burden, 4-days before sacrificing them (Fig. 5a). In this behavioral paradigm, the mice were habituated for 3 days and on the 4th day (testing day), a dish containing beddings from the homecage was placed in one end of the arena. During the pre-exposure phase, the mice explored the arena freely for 5 min (Fig. 5e, left). The animals were then confined to the bisect with the homecage beddings and the bobcat urine was introduced to the opposite bisect (Fig. 5e, right). The time spent in the homecage beddings bisect and the bobcat urine bisect during the 10 min "exposure phase" were recorded (Fig. 5e). During the pre-exposure stage, no difference in the time spent in the empty bisect was observed between the DMSO and UA-injected mice (Left: $t_{(8)} = 0.2658$, $p = 0.7971$; Right: $t_{(8)} = 0.3041$, $p = 0.7688$; Fig. 5f). However, upon introduction of the bobcat urine, UA-injected mice were less willing to leave the bisect containing their odor and spent less time in the cat odor bisect as compared to the DMSO control mice (Left: $t_{(8)} = 2.901$, $p = 0.0199$; Right: $t_{(8)} = 2.633$, $p = 0.03$; Fig. 5g). Since reduced aversion towards cat odor in chronically infected mice is known to correlate with the severity of the brain cyst load (Afonso et al., 2012; Evans et al., 2014; Xiao et al., 2016; Boillat et al., 2020), the altered innate response observed in the UA-injected mice provided additional evidence to support the reduced brain cyst burden in these animals (Fig. 5d).

4. Discussion

Toxoplasmosis continues to be a health threat to the world's population (Furtado et al., 2011). However, current drug regimens exhibit significant toxicity and are ineffective against the bradyzoite tissue cysts, counteracting efforts to fully eradicate the infection in patients (Dunay et al., 2018). Here, we demonstrate that PE and the metabolite UA negate neurotoxoplasmosis *in-vitro* by reducing tachyzoite load and inhibiting cyst formation. Additionally, this reduction in parasite burden is not a consequence of host cell cytotoxicity. Attenuation of proper cyst development by UA is also recapitulated *in-vivo*, where UA results in the formation of smaller brain cysts in the infected mice. Consequently, these animals displayed altered innate fear response towards cat odor. Together, our findings highlight the potential of dietary supplementation with functional foods enriched with UA as a natural remedy for acute and chronic toxoplasmosis. Additionally, our study supports the classical paradigm of host behavior manipulation by *T. gondii* in chronically infected rodents (Afonso et al., 2012; Evans et al., 2014; Xiao et al., 2016; Boillat et al., 2020), where the reduction in cyst burden observed with UA administration coincides with enhanced perceived risk towards predatory odors.

Physiologically active ingredients from plants and herbs are increasingly being recognized as sources of new drugs for the treatment of various human diseases, including toxoplasmosis (Sepulveda-Arias et al., 2014; Al Nasr et al., 2016; Arab-Mazar et al., 2017; Deng et al., 2019; Adeyemi et al., 2019). Compelling evidence over the years demonstrates the therapeutic effects of plant extracts against *T. gondii in-vitro* and *in-vivo* (Sepulveda-Arias et al., 2014; Al Nasr et al., 2016; Arab-Mazar et al., 2017; Deng et al., 2019; Adeyemi et al., 2019). Pomegranate fruit is

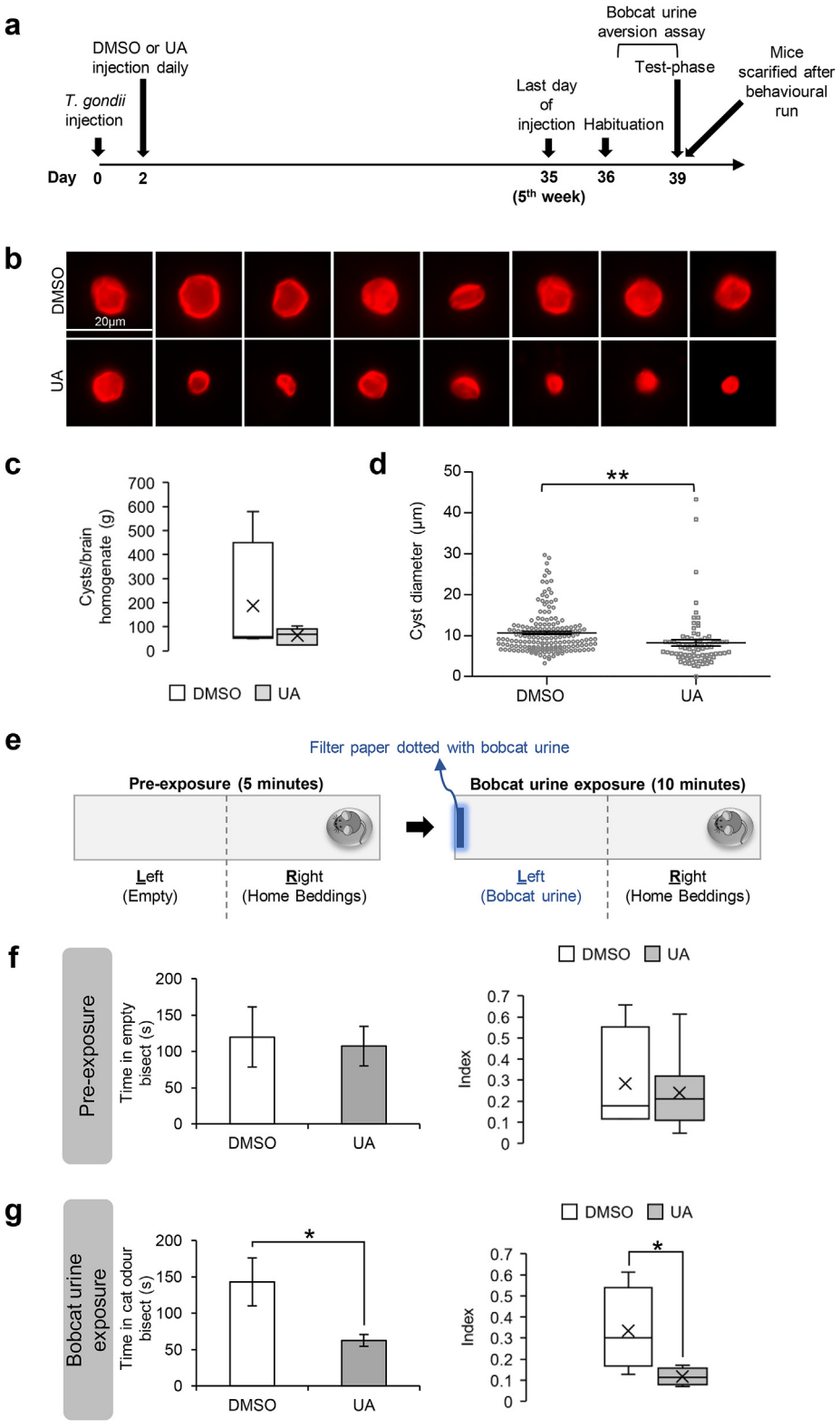

Fig. 5. Urolithin-A reduces brain cyst size and alters the innate response of infected mice towards cat odor. (a) Timepoints for the *in-vivo* workflow. (b) 8 representative images of brain cysts observed in infected mice administered with 30 μg UA or equivalent volume of DMSO. (c) Quantification of cyst count per gram of brain homogenate tabulated from 4 DMSO and 6 UA mice. The line inside the box represents the median and the cross (x) indicates the average. (d) Analysis of the diameter of cysts in the brains of infected animals. A total of 175 and 77 cysts were analyzed, tabulated from 4 DMSO and 6 UA mice, respectively. Each dot represents one cyst. The horizontal line represents the average diameter of the cysts. (e) Bobcat urine aversion assay behavioral paradigm. (f–g) Time spent in the left bisect (left) and the aversion index (right) during the pre-exposure and exposure phase. The aversion index is tabulated as $time_{left}/time_{right}$. The line inside the box represents the median and the cross (x) indicates the average. All values are mean ± S.E.M. Unpaired two-tailed t-test with a 95% confidence interval was performed. Differences against DMSO control are significant for $*p \leq 0.05$ and $**p \leq 0.001$. Scale bar: 20 μm.

widely regarded as a functional food that provides health benefits beyond basic nutrition (Johanningsmeier and Harris, 2011). Notably, UA, a gut microbiome-derived metabolite produced following pomegranate intake, is shown to be the bioactive molecule underlying the health benefits of pomegranate consumption (Espin et al., 2013). Here, our study provided evidence supporting dietary supplementation with PE or other UA-enriched food as a natural therapeutic alternative for neuroto xoplasmosis. Moreover, compared to the current standardized regimen of pyrimethamine and sulfonamides, PE and UA do not elicit *in-vitro* cytotoxicity.

Two other important factors need to be considered to ascertain the protective efficacy of dietary polyphenols against cerebral toxoplasmosis: the oral bioavailability and blood-brain barrier permeability. Polyphenols in diets are subjected to extensive metabolism in the gut;

whether these natural products can persist in the enterohepatic circulation to reach therapeutic concentration in the brain is still regarded with some reservations (Figueira et al., 2017; Teng and Chen, 2019). Apropos, gut-derived urolithins are shown to persist at high concentration in the bloodstream following pomegranate juice intake in human subjects and are blood-brain barrier permeable (Mertens-Talcott et al., 2006; Gasperotti et al., 2015; Yuan et al., 2016). These properties support UA as a physiologically relevant *in-vivo* compound to target toxoplasmosis in the brain. Nonetheless, additional optimization is needed to derive formulations that can achieve sustained concentration in the brain.

T. gondii disseminates as fast replicating tachyzoites to cause acute infection followed by differentiation into bradyzoites to form quiescent cysts that underlie human chronic infection (Dubey et al., 1998; Dubey, 2020). These cysts can be reactivated, releasing parasites that can convert into invasive tachyzoites to cause serious morbidity and mortality in immunocompromised patients (Frenkel and Escajadillo, 1987; Nissapatorn et al., 2004). However, the current first-line drugs can only suppress the replication of tachyzoites and are ineffective against the bradyzoite stage. Emerging studies have identified several natural compounds that can negate the brain cyst burden in murine toxoplasmosis (Dahbi et al., 2010; Schultz et al., 2014; Doggett et al., 2012; Bottari et al., 2015a, 2015b, 2016; Eraky et al., 2016; Azami et al., 2018; Spalenka et al., 2020). Here, our study identifies UA as a novel compound that can interfere with cyst formation *in-vitro* and *in-vivo*. Although the treatment paradigm used in our study was not sufficient to completely eradicate cyst burden, UA suppressed the formation and led to the appearance of smaller cysts. It should be noted, however, that the reduction in tachyzoite load by UA might have caused a prophylactic effect and hence, the downstream propensity of the parasites to form cysts in our murine infection model. Apropos, *in-vivo* experiments involving UA administration only at the chronic infection phase will more accurately delineate the effect of PE on the cyst burden independently of the tachyzoite load.

Several targets have been proposed to underlie the anti-*T. gondii* activity of plant-derived natural products. These include interference of the parasite DNA synthesis, RNA degradation, mitochondrial function, lipid metabolism, glyoxalase pathway, calcium homeostasis, cytoskeleton integrity, and locomotion (Doggett et al., 2012; Nagamune et al., 2007; De Pablos et al., 2010; Goo et al., 2015; Alday et al., 2017; Si et al., 2018; McConnell et al., 2018; Luan et al., 2019; Leesombun et al., 2020; Deng et al., 2020). Pro-oxidant effect to induce oxidative stress and DNA damage in the parasite has also been suggested (Gopalakrishnan and Kumar, 2015; Adeyemi et al., 2020). In addition to direct parasiticidal activity, modulation of host intracellular responses by natural phenolic compounds to cope with the infection have also been proposed (Ietta et al., 2017; Lee et al., 2020). Notably, the upregulation of host autophagy pathway is reported to inhibit *T. gondii* growth (Lee et al., 2020). Interestingly, the induction of *T. gondii* intrinsic autophagy activity has also been shown to interfere with tachyzoite to bradyzoite transformation (Li et al., 2016). PE and UA are known to harbor autophagy-inducing activity (Ryu et al., 2016; Tan et al., 2019). Indeed, this property underlies the neuroprotective effect of UA against ischemic neuronal injury and neuroinflammation *in-vivo* (Ahsan et al., 2019; Velagapudi et al., 2019). While our study did not delineate the mechanism underlying the anti-*T. gondii* effect of PE and UA on tachyzoite growth and cyst formation, it is possible that the autophagy-inducing property might in part, contribute to the attenuation of parasite burden observed in this study. Nevertheless, more studies are essential to critically decipher the mechanism underlying PE and UA actions on *T. gondii* infection.

Infection by *T. gondii* can alter the behavior of the intermediate hosts. Notably, infected rodents exhibit a reduced aversion to felid predators, possibly to increase predation and reproductive fitness of the parasites (Berdoy et al., 2000; Vyas et al., 2007; Vyas, 2015). Studies have reported that the altered fear response is associated with the neuroendocrine axis and the brain cyst burden (Afonso et al., 2012; Evans et al., 2014; Xiao et al., 2016; Boillat et al., 2020; Tong et al., 2019). More recently, neuroinflammation is shown to tightly correlate with the cyst load and both factors contribute to the severity of the behavioral alteration (Boillat et al., 2020). Here, our study demonstrates that the smaller cyst structures observed with UA administration coincide with an increased perceived risk of the infected mice towards cat odor. Hence, we postulate that the altered behavior is due to the reduction in brain cyst burden in the UA-injected mice. However, it is also important to examine the effect of UA on uninfected animals to exclude the possibility that the behavioral change is due to UA exclusively independent of *T. gondii* infection. Additionally, it should be noted that UA harbors anti-neuroinflammatory properties (Gong et al., 2019; Xu et al., 2018; DaSilva et al., 2019; Lee et al., 2019). Whether this anti-inflammatory characteristic could be a confounding variable that influences the behavioral outcome of the UA-injected mice should be investigated.

Defensive traits are important for survival and are innately expressed in many species. The polyphenol production in plants is itself a form of chemical defense against herbivory and microbial pathogens (Mayer, 2006). Plant-derived polyphenols are often used by primary consumers to sequester and use these in their chemical arsenal. A large body of literature suggests that such repurposing of plant polyphenols can have tri-trophic influences on prey-predator relationships between primary and secondary consumers (Sun et al., 2019; Sentis et al., 2019; Boege et al., 2019). Thus, it will be interesting to explore if the effect of UA has ecological relevance for the immunity of wildlife rodents to *T. gondii* infection and consequently, the consumption rates by their felid predators.

The identification of new remedies for the treatment of cerebral toxoplasmosis is important. Together, our study demonstrates the potential of dietary supplementation with functional foods enriched with UA as a natural remedy to combat neurotoxoplasmosis. Our findings are new and promising, highlighting a safer and cheaper alternative to current therapeutic regimens to mitigate acute and chronic *T. gondii* infection in humans.

Authors contributions

S.T. designed and carried out the experiments; W.H.T helped with the maintenance of *T. gondii* strain in culture, intraperitoneal injection and bobcat urine aversion behavior assay; S.T. and A.V. prepared the manuscript; A.V. supervised the entire research. All authors approved the final manuscript.

Declaration of competing interest

The authors declare that they have no known competing financial interests or personal relationships that could have appeared to influence the work reported in this paper.

Acknowledgement

This work was financially supported by Human Frontier Science Program (RGP0062/2018) and by the Ministry of Education, Singapore, under its MOE AcRF Tier 3 Award MOE2017-T3-1-002.

Appendix A. Supplementary data

Supplementary data to this article can be found online at https://doi.org/10.1016/j.bbih.2020.100128.

References

Adeyemi, O.S., et al., 2019. Focus: Organelles: in vitro screening to identify anti-toxoplasma compounds and in silico modeling for bioactivities and toxicity. Yale J. Biol. Med. 92 (3), 369.

Adeyemi, O.S., et al., 2020. Altered redox status, DNA damage and modulation of L-tryptophan metabolism contribute to antimicrobial action of curcumin. Heliyon 6 (3), e03495.
Afonso, C., Paixão, V.B., Costa, R.M., 2012. Chronic Toxoplasma infection modifies the structure and the risk of host behavior. PloS One 7 (3).
Ahsan, A., et al., 2019. Urolithin A-activated autophagy but not mitophagy protects against ischemic neuronal injury by inhibiting ER stress in vitro and in vivo. CNS Neurosci. Ther. 25 (9), 976–986.
Al Nasr, I., et al., 2016. Toxoplasmosis and anti-Toxoplasma effects of medicinal plant extracts-A mini-review. Asian Pac. J. Trop. Med. 9 (8), 730–734.
Alday, P.H., Doggett, J.S., 2017. Drugs in development for toxoplasmosis: advances, challenges, and current status. Drug Des. Dev. Ther. 11, 273.
Alday, P.H., et al., 2017. Genetic evidence for cytochrome b Qi site inhibition by 4 (1H)-quinolone-3-diarylethers and antimycin in Toxoplasma gondii. Antimicrob. Agents Chemother. 61 (2) e01866-16.
Andreux, P.A., et al., 2019. The mitophagy activator urolithin A is safe and induces a molecular signature of improved mitochondrial and cellular health in humans. Nat. Metabol. 1 (6), 595–603.
Arab-Mazar, Z., Kheirandish, F., Rajaeian, S., 2017. Anti-toxoplasmosis activity of herbal medicines: narrative review. Herb. Med. J. 2 (1), 43–49.
Azami, S.J., et al., 2018. Curcumin nanoemulsion as a novel chemical for the treatment of acute and chronic toxoplasmosis in mice. Int. J. Nanomed. 13, 7363.
Berdoy, M., Webster, J.P., Macdonald, D.W., 2000. Fatal attraction in rats infected with Toxoplasma gondii. Proc. Roy. Soc. Lond. B Biol. Sci. 267 (1452), 1591–1594.
Blader, I.J., et al., 2015. Lytic cycle of Toxoplasma gondii: 15 years later. Annu. Rev. Microbiol. 69, 463–485.
Boege, K., Agrawal, A.A., Thaler, J.S., 2019. Ontogenetic strategies in insect herbivores and their impact on tri-trophic interactions. Curr. Opin. Insect Sci. 32, 61–67.
Boillat, M., et al., 2020. Neuroinflammation-associated aspecific manipulation of mouse predator fear by toxoplasma gondii. Cell Rep. 30 (2), 320–334. e6.
Bottari, N.B., et al., 2015a. Sulfamethoxazole-trimethoprim associated with resveratrol for the treatment of toxoplasmosis in mice: influence on the activity of enzymes involved in brain neurotransmission. Microb. Pathog. 79, 17–23.
Bottari, N.B., et al., 2015b. Effects of sulfamethoxazole-trimethoprim associated to resveratrol on its free form and complexed with 2-hydroxypropyl-β-cyclodextrin on cytokines levels of mice infected by Toxoplasma gondii. Microb. Pathog. 87, 40–44.
Bottari, N.B., et al., 2016. Synergistic effects of resveratrol (free and inclusion complex) and sulfamethoxazole-trimetropim treatment on pathology, oxidant/antioxidant status and behavior of mice infected with Toxoplasma gondii. Microb. Pathog. 95, 166–174.
Cabral, C.M., et al., 2016. Neurons are the primary target cell for the brain-tropic intracellular parasite Toxoplasma gondii. PLoS Pathog. 12 (2).
Cerdá, B., et al., 2003. Evaluation of the bioavailability and metabolism in the rat of punicalagin, an antioxidant polyphenol from pomegranate juice. Eur. J. Nutr. 42 (1), 18–28.
Cerdá, B., et al., 2004. The potent in vitro antioxidant ellagitannins from pomegranate juice are metabolised into bioavailable but poor antioxidant hydroxy-6H-dibenzopyran-6-one derivatives by the colonic microflora of healthy humans. Eur. J. Nutr. 43 (4), 205–220.
Chen, P., et al., 2019. Activation of the miR-34a-mediated SIRT1/mTOR signaling pathway by urolithin A attenuates d-galactose-induced brain aging in mice. Neurotherapeutics 1–14.
Choi, S.H., et al., 2014. A three-dimensional human neural cell culture model of Alzheimer's disease. Nature 515 (7526), 274–278.
Dahbi, A., et al., 2010. The effect of essential oils from Thymus broussonetii Boiss on transmission of Toxoplasma gondii cysts in mice. Parasitol. Res. 107 (1), 55–58.
Dannemann, B., et al., 1992. Treatment of toxoplasmic encephalitis in patients with AIDS: a randomized trial comparing pyrimethamine plus clindamycin to pyrimethamine plus sulfadiazine. Ann. Intern. Med. 116 (1), 33–43.
DaSilva, N.A., et al., 2019. Pomegranate ellagitannin-gut microbial-derived metabolites, urolithins, inhibit neuroinflammation in vitro. Nutr. Neurosci. 22 (3), 185–195.
De Pablos, L.M., et al., 2010. Action of a pentacyclic triterpenoid, maslinic acid, against Toxoplasma gondii. J. Nat. Prod. 73 (5), 831–834.
Deng, Y., et al., 2019. Recent progress on anti-Toxoplasma drugs discovery: design, synthesis and screening. Eur. J. Med. Chem., 111711
Deng, H., et al., 2020. Synthesis, in vitro and in vivo biological evaluation of dihydroartemisinin derivatives with potential anti-Toxoplasma gondii agents. Bioorg. Chem. 94, 103467.
Doggett, J.S., et al., 2012. Endochin-like quinolones are highly efficacious against acute and latent experimental toxoplasmosis. Proc. Natl. Acad. Sci. Unit. States Am. 109 (39), 15936–15941.
Donato, R., et al., 2007. Differential development of neuronal physiological responsiveness in two human neural stem cell lines. BMC Neurosci. 8 (1), 36.
Dubey, J.P., 2016. Toxoplasmosis of Animals and Humans. CRC press.
Dubey, J.P., 2020. The history and life cycle of Toxoplasma gondii. In: Toxoplasma Gondii. Elsevier, pp. 1–19.
Dubey, J., Lindsay, D., Speer, C., 1998. Structures of Toxoplasma gondiitachyzoites, bradyzoites, and sporozoites and biology and development of tissue cysts. Clin. Microbiol. Rev. 11 (2), 267–299.
Dunay, I.R., et al., 2018. Treatment of toxoplasmosis: historical perspective, animal models, and current clinical practice. Clin. Microbiol. Rev. 31 (4) e00057-17.
Eraky, M.A., et al., 2016. Effects of Thymus vulgaris ethanolic extract on chronic toxoplasmosis in a mouse model. Parasitol. Res. 115 (7), 2863–2871.
Espin, J.C., et al., 2013. Biological significance of urolithins, the gut microbial ellagic Acid-derived metabolites: the evidence so far. Evid. Based Complement Alternat. Med. 2013, 270418.
Evans, A.K., et al., 2014. Patterns of Toxoplasma gondii cyst distribution in the forebrain associate with individual variation in predator odor avoidance and anxiety-related behavior in male Long–Evans rats. Brain Behav. Immun. 37, 122–133.
Fabiani, S., et al., 2015. Neurobiological studies on the relationship between toxoplasmosis and neuropsychiatric diseases. J. Neurol. Sci. 351 (1–2), 3–8.
Farha, M.A., Brown, E.D., 2016. Strategies for target identification of antimicrobial natural products. Nat. Prod. Rep. 33 (5), 668–680.
Ferguson, D., Hutchison, W., 1987. An ultrastructural study of the early development and tissue cyst formation of Toxoplasma gondii in the brains of mice. Parasitol. Res. 73 (6), 483–491.
Ferguson, D., Hutchison, W., Pettersen, E., 1989. Tissue cyst rupture in mice chronically infected with Toxoplasma gondii. Parasitol. Res. 75 (8), 599–603.
Figueira, I., et al., 2017. Polyphenols journey through blood-brain barrier towards neuronal protection. Sci. Rep. 7 (1), 1–16.
Frenkel, J., Escajadillo, A., 1987. Cyst rupture as a pathogenic mechanism of toxoplasmic encephalitis. Am. J. Trop. Med. Hyg. 36 (3), 517–522.
Frenkel, J., Dubey, J., Miller, N.L., 1970. Toxoplasma gondii in cats: fecal stages identified as coccidian oocysts. Science 167 (3919), 893–896.
Furtado, J.M., et al., 2011. Toxoplasmosis: a global threat. J. Global Infect. Dis. 3 (3), 281.
Gasperotti, M., et al., 2015. Fate of microbial metabolites of dietary polyphenols in rats: is the brain their target destination? ACS Chem. Neurosci. 6 (8), 1341–1352.
Gong, Z., et al., 2019. Urolithin A attenuates memory impairment and neuroinflammation in APP/PS1 mice. J. Neuroinflammation 16 (1), 62.
Goo, Y.-K., et al., 2015. Characterization of Toxoplasma gondii glyoxalase 1 and evaluation of inhibitory effects of curcumin on the enzyme and parasite cultures. Parasites Vectors 8 (1), 654.
Gopalakrishnan, A.M., Kumar, N., 2015. Antimalarial action of artesunate involves DNA damage mediated by reactive oxygen species. Antimicrob. Agents Chemother. 59 (1), 317–325.
Guo, M., et al., 2015. Prevalence and risk factors for Toxoplasma gondii infection in meat animals and meat products destined for human consumption. J. Food Protect. 78 (2), 457–476.
Gyawali, R., Ibrahim, S.A., 2014. Natural products as antimicrobial agents. Food Contr. 46, 412–429.
Hoffrogge, R., et al., 2006. 2-DE proteome analysis of a proliferating and differentiating human neuronal stem cell line (ReNcell VM). Proteomics 6 (6), 1833–1847.
Ietta, F., et al., 2017. Rottler in-mediated inhibition of Toxoplasma gondii growth in BeWo trophoblast-like cells. Sci. Rep. 7 (1), 1–9.
Jeffers, V., et al., 2018. A latent ability to persist: differentiation in Toxoplasma gondii. Cell. Mol. Life Sci. 75 (13), 2355–2373.
Johanningsmeier, S.D., Harris, G.K., 2011. Pomegranate as a functional food and nutraceutical source. Annu. Rev. Food Sci. Technol. 2, 181–201.
Katlama, C., et al., 1996. Pyrimethamine-clindamycin vs. pyrimethamine-sulfadiazine as acute and long-term therapy for toxoplasmic encephalitis in patients with AIDS. Clin. Infect. Dis. 22 (2), 268–275.
Kijlstra, A., Jongert, E., 2008. Control of the risk of human toxoplasmosis transmitted by meat. Int. J. Parasitol. 38 (12), 1359–1370.
Koshy, A.A., et al., 2010. Toxoplasma secreting Cre recombinase for analysis of host-parasite interactions. Nat. Methods 7 (4), 307.
Koshy, A.A., Harris, T.H., Lodoen, M.B., 2020. Cerebral toxoplasmosis. In: Toxoplasma Gondii. Elsevier, pp. 1043–1073.
Kujawska, M., et al., 2020. Neuroprotective effects of pomegranate juice against Parkinson's disease and presence of ellagitannins-derived metabolite—urolithin A—in the brain. Int. J. Mol. Sci. 21 (1), 202.
Lee, G., et al., 2019. Anti-inflammatory and antioxidant mechanisms of urolithin B in activated microglia. Phytomedicine 55, 50–57.
Lee, J., et al., 2020. 4-Hydroxybenzaldehyde restricts the intracellular growth of toxoplasma gondii by inducing SIRT1-mediated autophagy in macrophages. Kor. J. Parasitol. 58 (1), 7.
Leesombun, A., et al., 2020. Metacytofil in is a potent therapeutic drug candidate for toxoplasmosis. J. Infect. Dis. 221 (5), 766–774.
Li, X., et al., 2016. Induction of autophagy interferes the tachyzoite to bradyzoite transformation of Toxoplasma gondii. Parasitology 143 (5), 639–645.
Lindsay, D.S., Dubey, J.P., 2020. Toxoplasmosis in wild and domestic animals. In: Toxoplasma Gondii. Elsevier, pp. 293–320.
Luan, T., et al., 2019. Synthesis and biological evaluation of ursolic acid derivatives bearing triazole moieties as potential anti-Toxoplasma gondii agents. J. Enzym. Inhib. Med. Chem. 34 (1), 761–772.
Mayer, A.M., 2006. Polyphenol oxidases in plants and fungi: going places? Rev. Phytochem. 67 (21), 2318–2331.
McCarthy, M., 2015. Drug's 5000% Price Rise Puts Spotlight on Soaring US Drug Costs. British Medical Journal Publishing Group.
McConnell, E.V., et al., 2018. Targeted structure–activity analysis of endochin-like quinolones reveals potent qi and qo site inhibitors of toxoplasma gondii and plasmodium falciparum cytochrome bc 1 and identifies ELQ-400 as a remarkably effective compound against acute experimental toxoplasmosis. ACS Infect. Dis. 4 (11), 1574–1584.
McLeod, R., et al., 2020. Human toxoplasma infection. In: Toxoplasma Gondii. Elsevier, pp. 117–227.
Melzer, T., et al., 2010. Host cell preference of Toxoplasma gondii cysts in murine brain: a confocal study. J. Neuroparasitol. 1.
Mertens-Talcott, S.U., et al., 2006. Absorption, metabolism, and antioxidant effects of pomegranate (punica granatum L.) polyphenols after ingestion of a standardized extract in healthy human volunteers. J. Agric. Food Chem. 54 (23), 8956–8961.
Miller, N.L., Frenkel, J., Dubey, J., 1972. Oral infections with Toxoplasma cysts and oocysts in felines, other mammals, and in birds. J. Parasitol. 928–937.

Molan, A., et al., 2019. Global status of Toxoplasma gondii infection: systematic review and prevalence snapshots. Trop. Biomed. 36 (4), 898–925.
Nagamune, K., Beatty, W.L., Sibley, L.D., 2007. Artemisinin induces calcium-dependent protein secretion in the protozoan parasite Toxoplasma gondii. Eukaryot. Cell 6 (11), 2147–2156.
Nissapatorn, V., et al., 2004. Toxoplasmosis in HIV/AIDS patients: a current situation. Jpn. J. Infect. Dis. 57 (4), 160–165.
Parlog, A., Schlüter, D., Dunay, I.R., 2015. Toxoplasma gondii-induced neuronal alterations. Parasite Immunol. 37 (3), 159–170.
Porter, S.B., Sande, M.A., 1992. Toxoplasmosis of the central nervous system in the acquired immunodeficiency syndrome. N. Engl. J. Med. 327 (23), 1643–1648.
Remington, J.S., Cavanaugh, E.N., 1965. Isolation of the encysted form of Toxoplasma gondii from human skeletal muscle and brain. N. Engl. J. Med. 273 (24), 1308–1310.
Ryu, D., et al., 2016. Urolithin A induces mitophagy and prolongs lifespan in C. elegans and increases muscle function in rodents. Nat. Med. 22 (8), 879–888.
Schultz, T.L., et al., 2014. A thiazole derivative of artemisinin moderately reduces Toxoplasma gondii cyst burden in infected mice. J. Parasitol. 100 (4), 516–521.
Seeram, N.P., et al., 2006. Pomegranate juice ellagitannin metabolites are present in human plasma and some persist in urine for up to 48 hours. J. Nutr. 136 (10), 2481–2485.
Sentis, A., et al., 2019. Different phenotypic plastic responses to predators observed among aphid lineages specialized on different host plants. Sci. Rep. 9 (1), 9017.
Sepulveda-Arias, J.C., Veloza, L.A., Mantilla-Muriel, L.E., 2014. Anti-Toxoplasma activity of natural products: a review. Recent Pat. Anti-Infect. Drug Discov. 9 (3), 186–194.
Severance, E.G., et al., 2016. Toxoplasma gondii—a gastrointestinal pathogen associated with human brain diseases. In: International Review of Neurobiology. Elsevier, pp. 143–163.
Si, H., et al., 2018. Licochalcone A: an effective and low-toxicity compound against Toxoplasma gondii in vitro and in vivo. Int. J. Parasitol.: Drugs Drug Resist. 8 (2), 238–245.
Spalenka, J., et al., 2020. *In* vitro and in vivo activity of anogeissus leiocarpa bark extract and isolated metabolites against toxoplasma gondii. Planta Med. 86, 294–302, 04.
Sullivan Jr., W.J., Jeffers, V., 2012. Mechanisms of Toxoplasma gondii persistence and latency. FEMS Microbiol. Rev. 36 (3), 717–733.
Sun, R., et al., 2019. Tritrophic metabolism of plant chemical defenses and its effects on herbivore and predator performance. Elife 8.
Tan, S., et al., 2019. Pomegranate activates TFEB to promote autophagy-lysosomal fitness and mitophagy. Sci. Rep. 9 (1), 1–18.
Teng, H., Chen, L., 2019. Polyphenols and bioavailability: an update. Crit. Rev. Food Sci. Nutr. 59 (13), 2040–2051.
Tenter, A.M., Heckeroth, A.R., Weiss, L.M., 2000. Toxoplasma gondii: from animals to humans. Int. J. Parasitol. 30 (12–13), 1217–1258.
Tong, W.H., Abdulai-Saiku, S., Vyas, A., 2019. Testosterone reduces fear and causes drastic hypomethylation of arginine vasopressin promoter in medial extended amygdala of male mice. Front. Behav. Neurosci. 13, 33.
Torgerson, P.R., Mastroiacovo, P., 2013. The global burden of congenital toxoplasmosis: a systematic review. Bull. World Health Organ. 91, 501–508.
Tyebji, S., et al., 2019. Toxoplasmosis: a pathway to neuropsychiatric disorders. Neurosci. Biobehav. Rev. 96, 72–92.
Velagapudi, R., et al., 2019. Induction of autophagy and activation of SIRT-1 deacetylation mechanisms mediate neuroprotection by the pomegranate metabolite urolithin A in BV2 microglia and differentiated 3D human neural progenitor cells. Mol. Nutr. Food Res. 63 (10), 1801237.
Vyas, A., 2015. Mechanisms of host behavioral change in Toxoplasma gondii rodent association. PLoS Pathog. 11 (7).
Vyas, A., et al., 2007. Behavioral changes induced by Toxoplasma infection of rodents are highly specific to aversion of cat odors. Proc. Natl. Acad. Sci. Unit. States Am. 104 (15), 6442–6447.
Webster, J.P., 2001. Rats, cats, people and parasites: the impact of latent toxoplasmosis on behaviour. Microb. Infect. 3 (12), 1037–1045.
Xiao, J., et al., 2016. Behavioral abnormalities in a mouse model of chronic toxoplasmosis are associated with MAG1 antibody levels and cyst burden. PLoS Neglected Trop. Dis. 10 (4).
Xu, J., et al., 2018. Urolithins attenuate LPS-induced neuroinflammation in BV2Microglia via MAPK, Akt, and NF-κB signaling pathways. J. Agric. Food Chem. 66 (3), 571–580.
Yuan, T., et al., 2016. Pomegranate's neuroprotective effects against alzheimer's disease are mediated by urolithins, its ellagitannin-gut microbial derived metabolites. ACS Chem. Neurosci. 7 (1), 26–33.